J. Phys. D: Appl. Phys. **33** (2000) 1410–1416. Printed in the UK PII: S0022-3727(00)10418-8

A self-activating high-voltage, high-energy crowbar

Steven M Turnbull, Scott J MacGregor, Fadhil A Tuema and Andrew J McPhee

Department of Electronic and Electrical Engineering, University of Strathclyde, 204 George Street, Glasgow G1 1XW, UK

E-mail: s.turnbull@eee.strath.ac.uk, s.macgregor@eee.strath.ac.uk, f.tuema@eee.strath.ac.uk and a.mcphee@eee.strath.ac.uk

Received 16 December 1999

Abstract. A self-closing crowbar switch has been designed and tested up to a voltage of 500 kV. The crowbar utilizes the consistent nature of electrical breakdown in water under highly non-uniform electric fields as the timing mechanism for closure and has no requirement for external triggering. The device can be operated with closure times which are controllable over the range 200–500 ns by altering the gap spacing of the switch electrodes. Measurements of the crowbar performance are presented, as well as the important aspects associated with the electrostatic design.

1. Introduction

In a number of high-voltage applications including pulsed μ-wave generation [1], the load need only be subjected to the high-voltage for a short period of time, possibly for less than 1 μs. Longer exposure to a high-voltage stress can often result in damage to the device being driven. This means that the pulse generator must produce the correct pulse length. Alternatively, the duration of the high voltage pulse may be controlled using a crowbar system. A crowbar system activates after a specified time delay and chops the high-voltage impulse, diverting the unwanted energy away from the device.

When driving high voltage loads with conventional Marx impulse generators, which produce a double exponential voltage profile, the duration of the wavetail of the Marx impulse can exceed the useful pulse length required by the load. In some cases, the long wavetail can be damaging to the load through an increased risk of electrical breakdown. Also, the long wavetail may result in excessive erosion of the electrodes as internal arcing may occur if the voltage is present for longer than is required. This can significantly reduce the lifetime of the device. Typical wavetails produced by this type of generator can be several microseconds in duration, and typical load pulse requirements may be as short as a few 100 nanoseconds. A crowbar system is therefore required in some situations to isolate the load at times after a few 100 nanoseconds.

The load of interest for this crowbar application operated at voltages up to 500 kV in magnitude, with pulse durations which were variable over the range 200–500 ns. If the pulse duration exceeded 500 ns, load cathode erosion would occur at an increased rate, which would reduce cathode lifetime. Also, the risk of a surface flashover within the load cavity increased significantly after 500 ns. A surface flashover could potentially damage the sensitive load cathode. A crowbar was therefore required to protect the load at times greater than 500 ns.

There are a number of high-voltage, high-energy crowbar systems published in the literature, which are based on a number of different switching mechanisms. These include the use of thyratrons [2], vacuum spark gaps [3] and gas-filled spark gaps [4–7]. The systems described have maximum operating voltages below 500 kV and are limited in terms of the energy which they can safely divert. A number of these are also relatively complex and expensive to build, and are not capable of responding in the short times of interest for this application. For these reasons, none of the existing systems were regarded as being suitable and it was decided to develop a crowbar switch that relied upon electrical breakdown in water.

The crowbar switch consisted of a non-uniform field electrode arrangement immersed in de-ionized water. The crowbar is self-activated by the application of the voltage impulse from the Marx generator that drives the load. This removes the requirement for a triggering mechanism. De-ionized water was used as the insulating material for two reasons. First, in the sub-microsecond timescale, water can withstand electric field strengths in the region of several 100 kilovolts per centimetre [8] and will therefore be able to readily switch voltage levels of 500 kV. Second, it has been reported throughout the literature that the arc formation process in water in a highly non-uniform electric field occurs in a temporally consistent manner [8–14]. This behaviour suggested the possibility of developing a crowbar switch which was self-activating, thus removing the requirement for triggering and maintaining the simplicity of the crowbar system.

In one investigation into water breakdown with a point–plane electrode geometry [9], the empirical formula derived from the data indicated that the average streamer velocity in water, and therefore the approximate time to gap closure, could be found from a knowledge of the gap spacing and the applied voltage. The relevant relationships are:

$$Dt^{-1/2} = 8.8V^{0.6} \qquad \text{(for a positive point electrode)}$$

$$Dt^{-2/3} = 16V^{1.1} \qquad \text{(for a negative point electrode)}$$

where D is the gap spacing in centimetres, t is the time taken for the streamer to cross the gap in microseconds, and V is the applied voltage in megavolts. These relationships indicate that the breakdown time of a water gap can be varied simply by changing either the applied voltage or the gap spacing. This provides a straightforward method of varying the delay time to crowbar action.

The relationships also show the polarity effect that is observed in water. The positive point water gap closes in a shorter time than the negative point case for the same applied voltage and gap spacing. Using the positive point relationship, the time taken for the streamer to bridge a gap of a few centimetres is calculated to be a few 100 nanoseconds. For example, a voltage of 300 kV applied to a gap of 3 cm should result in a streamer bridging the gap in 494 ns for positive point conditions. If the point is negative, the time taken for the streamer to bridge the gap is longer, at 590 ns. This means that the required delay times of between 200 and 500 ns are achievable for sensible gap spacings of a few centimetres, even allowing for the extra formation time of the conducting arc channel. It should therefore be possible to construct a switch which is of a practicable size.

2. Experimental details

As discussed above, electrical breakdown in water under intense non-uniform electric fields occurs with a streamer formation time which is reasonably consistent. It was therefore decided to use a rod–plane electrode configuration for the switch to generate the required field non-uniformity. The intense electric field around the point electrode will ensure that streamer initiation occurs rapidly after the voltage is applied. This rapid initiation of the streamer minimizes any statistical effects in the breakdown time of the water gap. The breakdown time is then dominated by the formation time of the arc channel. This has been reported as being reasonably consistent for similar average electric fields and gap lengths [8, 9].

It was decided to employ a positive point–negative plane polarity configuration, as the polarity effect mentioned before means that for a specific value of delay time to crowbar closure, the size of the water gap is minimized and the crowbar will therefore close, and isolate the load, in the fastest possible time. As the impulse voltage to be crowbarred was of a negative polarity, the high-voltage electrode was selected as the plane electrode and the point electrode was the earth electrode.

A schematic diagram of the passive crowbar switch is shown in figure 1. It consists of a rod–plane electrode configuration immersed in de-ionized water. The resistivity

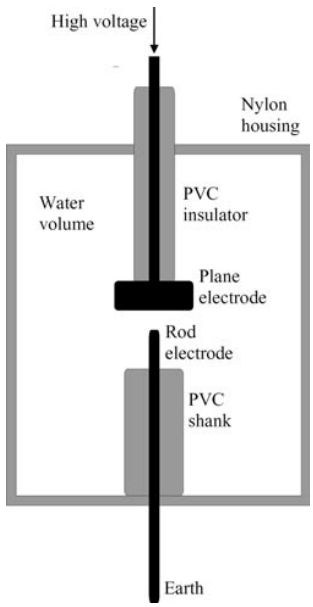

Figure 1. A schematic diagram of the water crowbar switch.

of the water was measured, following de-ionization and found to be 3 MΩ cm. The switch housing was cylindrical in shape with a diameter of 40 cm and a height of 70 cm. The wall thickness of the water container was 2 mm. The high-voltage plane electrode was 10 cm in diameter, with edges rounded to a radius of 1 cm. The rod earth electrode was 3 mm in diameter, 100 mm long and was tapered over a length of 1 cm to a final radius of 0.5 mm. The electrode gap spacing was variable between 10 mm and 70 mm. A 20 mm diameter PVC shank surrounded the rod electrode. The shank extended to within 30 mm of the rod tip and was included not only to support the rod electrode, but also to minimize the capacitive losses through the switch and to increase the switch resistance. The resistance between the rod and plane is increased by the presence of the PVC shank as it reduces the electrode surface area in contact with the water. This therefore minimizes resistive loading caused by the switch. The PVC shank also causes a significant alteration in the distribution of the electric field throughout the water volume and this reduces the voltage dropped across the switch. This in turn affects the capacitive loading experienced during pulse charging of the load.

The performance of the switch was measured using a ten stage Marx generator which produced negative impulse voltages up to a peak value of 700 kV in air. The output voltage pulse was double exponential in profile, with a nominal rise-time of 30 ns and a decay time to a half-peak value of 2 μs when loaded with an external tail resistor of 2 kΩ. A series de-coupling resistor of 100 Ω, constructed from aqueous $CuSO_4$ solution, was placed between the Marx output feed and the crowbar switch to limit the peak current from the generator during crowbar operation. The voltage applied to the crowbar was measured using an aqueous $CuSO_4$ voltage divider with input impedance of 2 kΩ. The response time of the divider was 25 ns and its maximum operating voltage exceeded 700 kV. A circuit diagram of the experimental system is shown in figure 2. The estimated inductance of the Marx

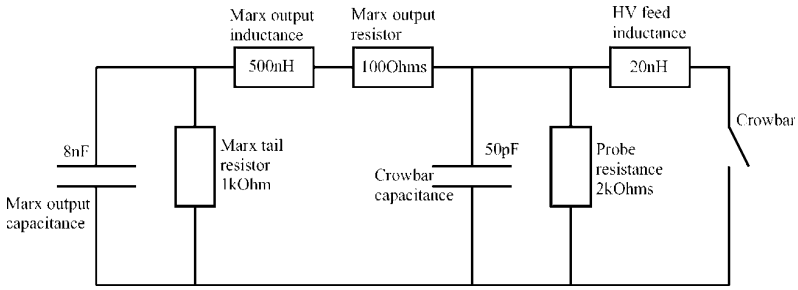

Figure 2. The circuit used to characterize the water crowbar switch.

generator output feed (500 nH) and the crowbar high-voltage connection (20 nH) are included. The self-capacitance of the crowbar was calculated using an electrostatic analysis programme [15] and was found to be approximately 50 pF. This is also included in the circuit diagram.

3. Electrostatic modelling

When using water as an insulating material, attention must be given to the electric field distribution in and around the water volume. The high permittivity of water ($\varepsilon_r = 80$) relative to air and the proximity of any grounded surface can significantly affect the electric field distribution. Also, the self-capacitance of the water volume can be significant and this can capacitively load the source generator, reducing the obtainable output voltage.

The electric field distribution in and around the crowbar switch was calculated using a 2D electrostatic analysis programme [15], which used a rotationally symmetric model of the switch. The switch model was positioned at a height of 350 mm above a conducting earth plane and the PVC shank surrounding the rod electrode was assigned a permittivity of $\varepsilon_r = 4$. The distribution of equipotentials is shown in figure 3(*a*). For 1 V applied to the plane electrode and an electrode gap spacing of 55 mm, the peak electric field at the rod tip was found to be 7.5 V cm^{-1} and the average field in the gap was 0.182 V cm^{-1}. The field enhancement factor for the model is therefore 41.2. For an applied voltage of 500 kV, the peak electric field at the rod tip is nominally 3.75 MV cm^{-1}. This value was considered high enough to ensure rapid initiation of the breakdown process. The actual peak electric field at the rod tip will vary as a result of changes in the gap spacing and erosion of the rod tip.

It can also be seen from figure 3(*a*) that 70% of the applied voltage appears along the underside of the crowbar switch. If the applied voltage is 500 kV, this represents a voltage of 350 kV appearing in air on the outer surface of the water container. There is therefore a significant risk of surface flashover across the switch body and flashover to earth. Another problem which was found in the analysis was the bunching of equipotentials inside the PVC shank surrounding the rod electrode. This reveals the presence of a significant potential gradient through the PVC shank that may result in breakdown of the shank. It may also lead to puncturing of the vessel at the point at which the rod electrode enters the water volume. It can be seen from figure 3(*a*) that around 60% of the applied voltage appears on the surface of the PVC shank. At the maximum operating voltage of 500 kV, a voltage of about 300 kV will appear on the outer surface of the shank, the inner surface remaining at 0 V. The average electric field in the PVC is therefore 350 kV cm^{-1}. This may result in breakdown of the PVC even though the applied voltage is only present for a few 100 nanoseconds. Bunching of the equipotentials also occurs around the rod as it exits the water volume. This region may therefore be prone to surface discharges and possible puncturing of the switch housing.

One method of relieving the electrical stress in these regions is to completely remove the shank. The equipotential distribution for this case is shown in figure 3(*b*). It can be seen that both potential problems have been alleviated. There is no bunching of the equipotential lines in the region where the rod electrode enters the vessel, and now only 50% of the applied voltage appears along the underside of the switch. This significantly reduces the risk of flashover as insulation requirements are known to increase nonlinearly with voltage [8]. However, the presence of the PVC shank did serve to reduce the resistive and capacitive losses through the switch. The redistribution of equipotentials after removal of the shank indicates that there is now a higher percentage of the applied voltage distributed across the water volume (50% as opposed to 30%). This will result in a significant increase in the loading that takes place during charging of the switch. Although not quantified here, it is reasonable to infer that the switch resistance will be reduced by the removal of the PVC shank. The complete length of the rod electrode will be exposed to the water which will effectively increase the surface area of the electrodes and reduce the resistance between them. This will cause a reduction in the voltage appearing across the load as a result of the resistive division which occurs between the switch resistance and the Marx generator output resistor (100 Ω).

In order to minimize the capacitive loading caused by the switch, the PVC shank was redesigned to generate a similar equipotential distribution to that shown in figure 3(*b*). To achieve this, the shank is tapered outward from the rod tip end down to the switch base. The equipotential distribution for a switch with a tapered shank is shown in figure 3(*c*). It can be seen that the equipotential distribution along the underside of the switch is similar to that in figure 3(*b*) with no shank present, but now only 30% of the applied voltage appears across the switch, as is the case in figure 3(*a*). The tapered shank minimizes the capacitive loading incurred by the switch and also relieves the electric field stress along the base of the switch. This shank design was employed in the final crowbar design.

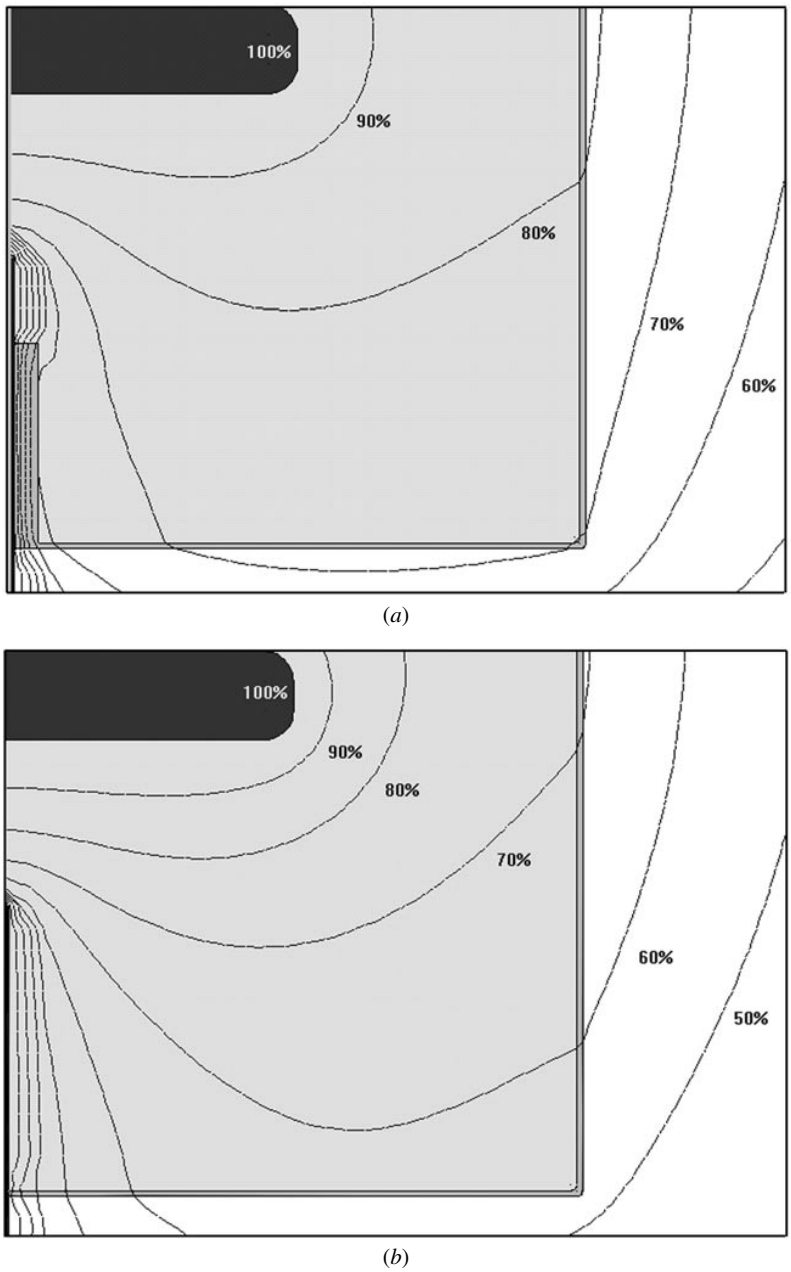

Figure 3. The equipotential distribution in and around the water crowbar switch, with (*a*) a cylindrical PVC shank surrounding the rod electrode; (*b*) no PVC shank surrounding the rod electrode and (*c*) a tapered PVC shank surrounding the rod electrode.

4. Crowbar timing measurements

An example of the crowbar switching performance is displayed in the composite oscillogram in figure 4. Here, 12 crowbarred output voltage waveforms from the Marx generator are superimposed on a single oscillogram. The risetime to the peak value of the Marx pulse has increased from a value of 30 ns when loaded with a 2 kΩ resistor, to a value of 100 ns (10–90%) when loaded with the crowbar switch. The self-capacitance of the switch causes this increase in risetime and also affects the voltage efficiency of the generator. Under the loaded condition, the peak voltage is 388 kV for a charging voltage of 50 kV. For no load, the Marx generator is 97% efficient at a charging voltage of 50 kV and would normally produce an output voltage of 485 kV. The loading caused by the crowbar reduced the voltage efficiency to 80%. For these waveforms, the average delay time to breakdown is 222 ns and the jitter in the delay time is 17 ns. The jitter was calculated as the standard deviation in the delay time values. The electrode spacing was 45 mm for these measurements. The crowbar closure time is observed to be 20–30 ns, which means that the load is rapidly isolated and protected. The 12 waveforms are consistent in profile and indicate that repeatable crowbar action is achievable using this method with a reasonably stable delay time to closure.

To determine the longer-term operation of the crowbar, the delay time to closure was measured over 80 consecutive shots with no maintenance of the electrodes. The applied voltage was 330 kV and the gap spacing was set to 35 mm.

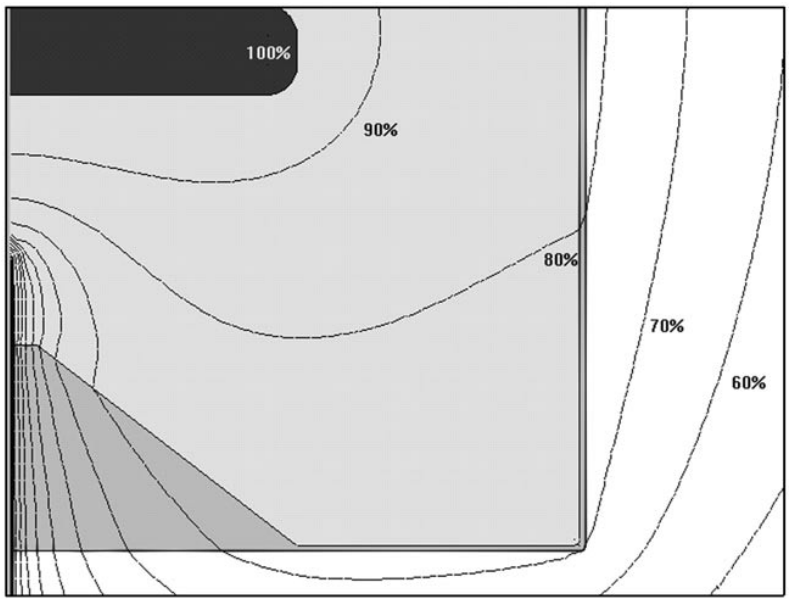

(*c*)

Figure 3. (Continued)

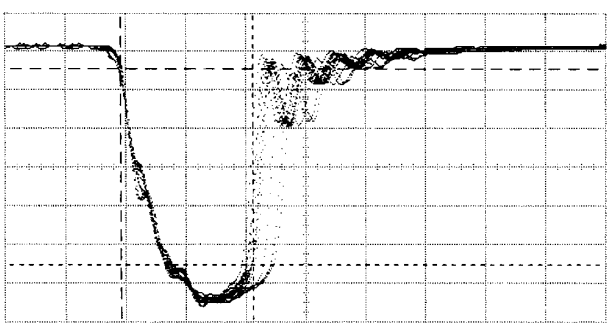

Figure 4. 12 superimposed Marx impulse waveforms. The peak voltage is 388 kV and the average time to crowbar closure is 222 ns with a jitter of 17 ns.

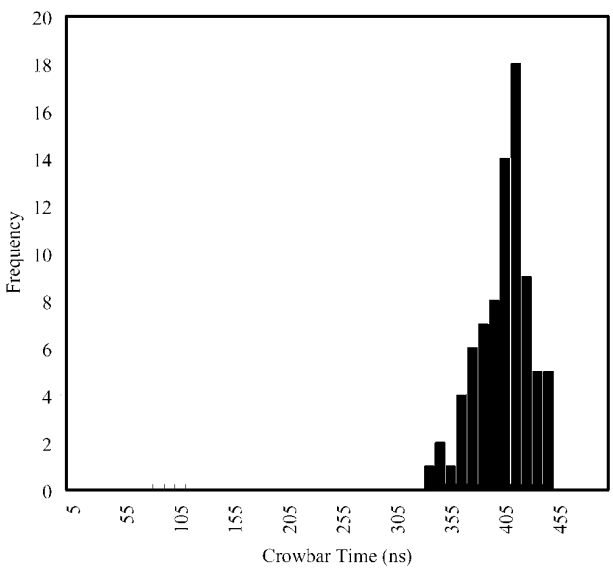

Figure 5. A histogram of the delay time values for 80 crowbar operations.

The results were plotted as a histogram and are shown in figure 5. The average time to crowbar closure was 403 ns and the jitter (standard deviation) was calculated to be 25 ns. This trial clearly establishes that reasonably consistent crowbar performance is achievable using a self-activating water gap.

The data from the trial was broken down into four segments of 20 shots in order to evaluate the effect of erosion of the point electrode on the delay time to closure. The drift in the delay time values is illustrated in figure 6, in which the average delay time values are plotted for each segment. It can be seen that the erosion of the point electrode causes a drift rate in the delay time of about 5 ns per 20 shots. The jitter values for each of the average delay time values in figure 6 are shown in figure 7. It can be seen that the jitter maintains a reasonably constant value at around 25 ns.

In order to establish that the crowbar delay time could be readily altered, the performance of the crowbar switch was determined for delay times to closure of 200 and 400 ns. A voltage range of 100–500 kV was used and the gap spacing was varied over the range of 15–65 mm, in steps of 10 mm. For each value of electrode spacing, the applied voltages required to produce an average delay time of 200 and then 400 ns were recorded. The results were plotted to provide a characteristic of electrode spacing against applied voltage for each of the delay times to breakdown. These results are shown in figure 8. Each data point on the characteristics is taken from an average of 12 crowbar closures. It can be seen that both characteristics are reasonably linear over the voltage range of interest. Therefore, for a particular load operating voltage in the above range, a delay time of 200 or 400 ns can be selected by simply using the appropriate characteristic to determine the required gap spacing. Using this type of characteristic, which can be found readily for other values of delay time, it is possible to operate the crowbar over a

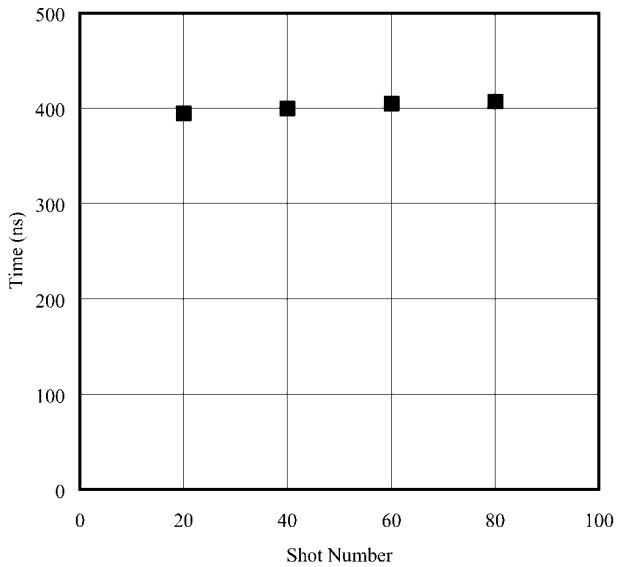

Figure 6. The drift in the delay time to crowbar closure, averaged for every 20 closures over 80 shots.

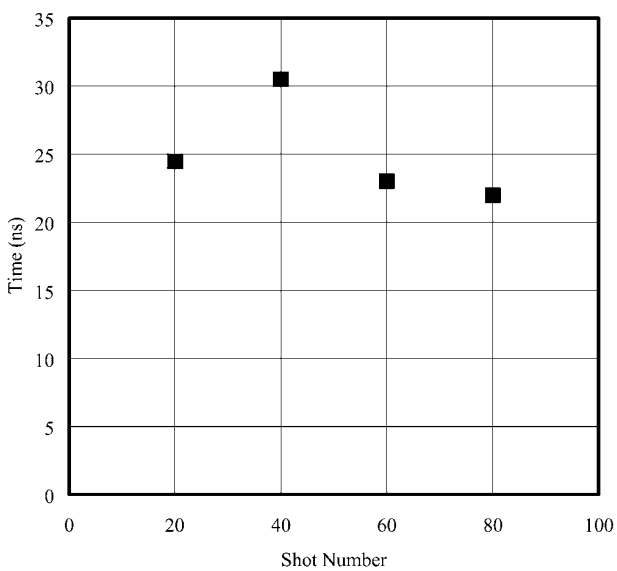

Figure 7. The jitter in the delay time to crowbar closure, averaged for every 20 closures over 80 shots.

wide range of voltages and alter the delay time to suit the application by simply altering the electrode gap spacing.

It can be seen from figure 8 that the rate of change of the delay time with applied electric field becomes significantly high as the gap spacing is increased from 15 to 55 mm. For example, at a gap spacing of 15 mm, a change in the electric field from 53 to 140 kV cm^{-1} results in a change in the delay time from 400 to 200 ns. In comparison, at a gap spacing of 55 mm, an increase in the field from 74 to 80 kV cm^{-1} was sufficient to obtain a similar reduction in delay time. This may be explained by a change in the dominant factor that controls the total delay time to breakdown of a water gap. This change takes place gradually as the gap spacing is increased. The delay time to breakdown of water is determined by the time required for a streamer to bridge the gap and, also, the formation time of the arc channel. It has been reported

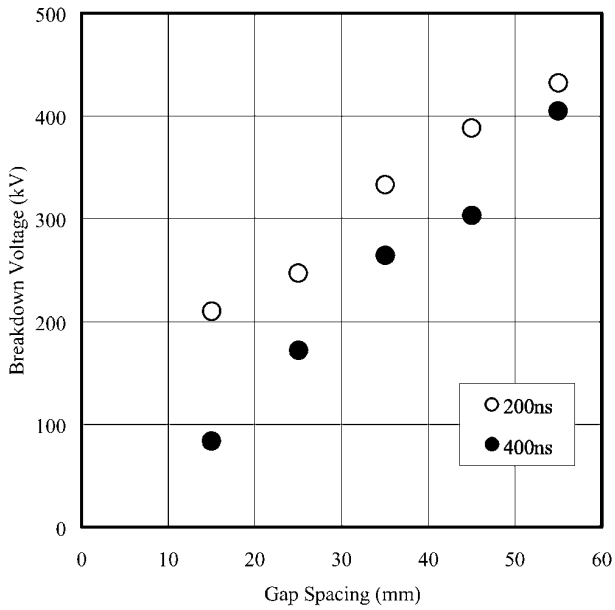

Figure 8. The crowbar closure characteristics for delay time values of 200 and 400 ns.

that the streamer transit time is highly dependent upon the average value of electric field in the gap [8]. This degree of dependency is much greater than that exhibited by the arc formation time. For a small gap spacing, it is possible that the streamer transit time is comparable to the arc formation time. As a result, the total delay time to breakdown will exhibit a moderate dependency on the average value of the applied field. As the gap spacing is increased, and the average electric field falls the streamer transit time becomes longer and therefore more dominant in determining the overall delay time to breakdown. This in turn makes the total delay time to breakdown highly field dependent. Therefore, it would become difficult to vary the delay time to crowbar closure for larger gap spacings as only slight changes in the applied voltage could result in large changes in the delay time.

5. Conclusions

The results obtained with a self-closing water crowbar clearly illustrate that it is quite possible to employ the consistent temporal nature of water breakdown for sub-microsecond crowbar operation in applications where timing is not overly critical. The crowbar developed for this study had a rod–plane electrode geometry immersed in de-ionized water, and this device demonstrated a delay time to closure which varied by only $\pm 6\%$ over a total of 80 shots (delay time = 403 ns, jitter = 25 ns).

A tapered PVC shank surrounding the rod electrode, was employed to reduce the capacitive loading caused by the switch. The profile of the shank was determined through electrostatic analysis. The shank also helped to reduce the risks of puncturing and surface flashover along the switch base.

The reliability of the crowbar is clearly illustrated in the histogram of figure 5 and the drift data in figure 6. The gradual drift in the delay time observed over eighty operations has been attributed to erosion of the rod electrode, which results

in an increase in the gap spacing. A solution to this problem would be to employ an electrode arrangement that generates a suitably non-uniform electric field and, also, possesses a much larger surface area. For example, the rod electrode could be replaced by a 'knife edge' shaped electrode which would still generate the required electric field distribution. This will result in a significant reduction in the rate of erosion of the non-uniform electrode with a corresponding reduction in the delay time drift. However, it can be seen from figure 7 that, even with electrode erosion, the jitter in the delay time is not significantly affected. The jitter remains reasonably constant at 25 ns over 80 operations.

Figure 8 illustrates the versatility of the crowbar switch over the voltage range 100–450 kV. The breakdown characteristics for 200 and 400 ns could be readily extended to cover a broader range of delay times, possibly up to a maximum delay time of 1 μs.

Acknowledgment

The authors wish to thank the DERA for their support of this work on contract WSF/U892.

References

[1] Miller R B 1997 Super reltrons and pulsed power issues *IEE Coll.—Pulsed Power '97 (Savoy Place, London)* Paper 8

[2] Nicholls N S, Menown H and Wheldon R J 1978 Double ended hydrogen thyratrons for crowbar protection of high power TWT systems *Proc. 13th Int. Pulsed Power Conf. (Buffalo NY, June 20–22, 1978)* pp 105–12

[3] Thompson J E, Fellers R G, Sudarshan T S and Warren F T 1980 Design of a triggered vacuum gap for crowbar operation *Proc. 14th Int. Power Modulator Symp. (Piscataway NJ, June 3–5, 1980)* pp 85–91

[4] Robinson J W 1980 Self-crowbarring, load isolating triggered spark gap *Rev. Sci. Instrum.* **51** 1532–4

[5] Mitre A K and Tellerico P J 1983 Spark gap crowbar for high voltage power supply *IEEE Trans. Nucl. Sci.* **30** 2862–4

[6] Hornkohl J O and Lynch M T 1988 Development of a high energy crowbar for the Los Alamos free electron laser *Nucl. Instrum. Meth. Phys. Res.* A **272** 227–31

[7] Higgins P B and Mathews F H 1979 Explosively triggered gas-dielectric crowbar switch *Rev. Sci. Instrum.* **50** 435–7

[8] Storr T H and Martin J C 1978 Interim notes on water breakdown *Report* SSWA/JCM/785/147 AWRE, Aldermaston, May

[9] Martin J C 1970 Nanosecond pulse techniques *Report* SSWA/JCM/704/49, AWRE, Aldermaston, April

[10] Sazama F J and Kenyon V L 1979 A streamer model for a high voltage water switch *Proc. 2nd IEEE Pulsed Power Conf. (Lubbock, June 12–14, 1979)* pp 187–90

[11] Jones H M and Kunhardt E E 1995 Development of pulsed dielectric breakdown in liquids *J. Phys. D: Appl. Phys.* **28** 178–88

[12] Jones H M and Kunhardt E E 1995 Prebreakdown currents in water and aqueous solutions and their influence on pulsed dielectric breakdown *J. Appl. Phys.* **78** 1–7

[13] Jones H M and Kunhardt E E 1995 Pulsed dielectric breakdown of pressurised water and salt solutions *J. Appl. Phys.* **77** 795–805

[14] Van Devender J P and Martin T H 1975 Untriggered water switch *IEEE Trans. Nucl. Sci.* **22** 979–82

[15] Integrated Engineering Software 1995 *2-D Electrostatic BEM Analysis Programme-ELECTRO* Winnipeg, Canada